

Towards Image Quality Analysis of Small and Full Field of View Dental Cone Beam CT Systems

E.C. Hoffmann¹, A.M. Marques da Silva² and D.F.G. Azevedo³

¹ PUCRS, Núcleo de Pesquisa em Imagens Médicas, Porto Alegre, Brazil

² PUCRS, Faculdade de Física, Porto Alegre, Brazil

³ PUCRS, Faculdade de Engenharia, Porto Alegre, Brazil

Abstract— Cone-beam CT (CBCT) systems have been used for dentomaxillofacial surgery applications. Different dental CBCT devices are being developed and released, with a wide variability of exposure parameters and fields of view. Although they have sufficient diagnostic quality, a quantitative analysis of image quality and radiation dose is required to enable their optimal use. The aim of this study was to develop and implement a feasible methodology for image quality analysis for different dental CBCT devices. The methodology was based on conventional CT quality control procedures and adapted to overcome the limitations of dental CBCT. A prototype phantom was specially designed to allow the acquisition of image quality parameters relevant to dental imaging. Equipments were divided into categories, related to their field of view: Small Field of View (SFOV) and Full Field of View (FFOV). The following image quality parameters were evaluated: uniformity, noise, contrast-to-noise ratio, CT number accuracy, artifacts, spatial resolution and geometric distortion. Applicability of the methodology was assessed using one SFOV and four FFOV CBCT devices. Results from preliminary analyses of the prototype phantom showed its potential for routine quality assurance on dental CBCT. Large differences in image quality performance were seen between the devices.

Keywords— Image Quality, Cone Beam CT, Dental Imaging, Phantom

I. INTRODUCTION

Over the past years, cone beam computed tomography (CBCT) imaging has been used in diagnostic radiology of the head and neck by dentists, orthopedists and otolaryngologists¹. This dental imaging modality is generally thought to offer a lower radiation dose and a higher spatial resolution than conventional multislice CT (MSCT), allowing a large degree of versatility in the reformatting of the dataset in orthogonal, oblique, or curved planes or as volumes². Some of the drawbacks of the dental CBCT devices are their inability of discriminating soft tissue because of its low contrast resolution, and the inaccuracy to give information about soft tissue quality³.

CBCT devices currently on the market have a variety of exposure parameters and field of view (FOV) sizes, which affect the image quality and the exposure dose. Although the same basic CT image acquisition principle is used by all of devices, different hardware and software, mainly related to the reconstruction algorithm, are used.

Standard quality control procedures for conventional CT are not fully applicable for CBCT devices. Commercial QC phantoms used for conventional CT, are not applicable for dental CBCT due to the difference in performance for certain image quality aspects. Furthermore, there is a lack of quantitative methods for image quality analysis suitable for dental CBCT, and it is difficult to establish ranges for these parameters, considering the lack of a general threshold or range for acceptable parameter values.

A variety of phantoms and test objects have been used in the evaluation of CBCT^{4,5}. However, it is difficult to relate technical image quality parameters to the clinical situation and to obtain threshold values for clinical use. There has been no wide-scale evaluation of the imaging performance of CBCT and the tools used for analysis are suboptimal, leading to results that are difficult to relate to the diagnostic performance.

The aim of this study is to develop and implement a feasible methodology for image quality analysis for different dental CBCT devices, allowing the measurement of parameters which are relevant to dental imaging requirements.

II. METHODS

A. Development of CBCT Phantom

To investigate the application of different image quality parameters for CBCT devices, a prototype phantom, called CBCT phantom, was specially designed to allow the acquisition of image quality parameters.

For this prototype, a head-size cylindrical polymethyl methacrylate (PMMA) phantom (160 mm diameter, 160 mm height) was designed with three sectors (Figure 1).

The phantom was designed based on previous work⁵,

devices, without reference levels for both technical and visual image-quality parameters.

CBCT phantom is divided into 3 sectors (Fig. 1). The first sector is designed to evaluate the CT number, contrast resolution, artifacts and spatial resolution. It consists of a PMMA cylinder (160 mm diameter, 20 mm height), with 7 cylindrical holes (35 mm diameter, 20 mm height) positioned at the center and vertices of a regular hexagon, where interchangeable cylindrical inserts containing different materials and structures are placed. The second sector is a uniform PMMA cylinder (160 mm diameter, 20 mm height), designed to evaluate the uniformity and noise. The third sector is composed by 6 PMMA cylinders (160 mm diameter, 20 mm height) with an array of regularly arranged small holes (4 mm diameter, 20 mm depth), designed to evaluate geometric distortion.

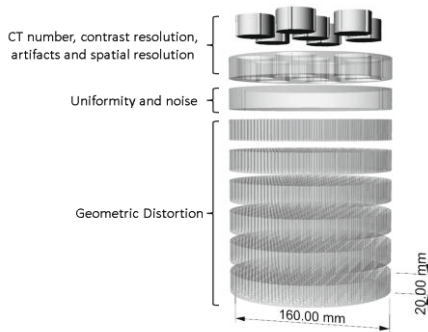


Fig. 1 CBCT phantom sectors and related image quality parameters.

Figure 2 shows CBCT phantom positioning at the FFOV-2 (9500 3D Kodak). A platform to assure the correct phantom alignment in CBCT devices was designed.

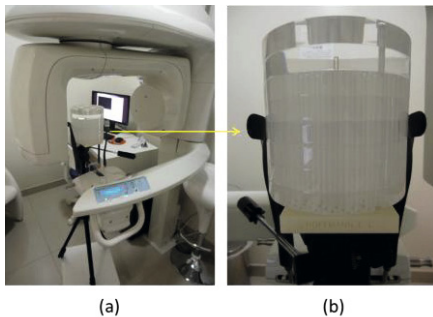


Fig. 2 CBCT phantom positioned at FFOV-2 (9500 3D Kodak).

B. Image Acquisition on MSCT and CBCT devices

Table 1 shows the exposure conditions used in this study. MSCT was used as reference for the image quality parameters, except for spatial resolution. Equipments were divided into categories for the analysis, related to their field of view:

Small Field of View (SFOV) and Full Field of View (FFOV). SSFOV are those equipments in which the field of view is limited to a volume smaller than the jaws (mandible and maxilla). Typically this refers to small fields of view suitable for imaging one, or a few teeth.

Table 1 Exposure parameters and physical characteristics of MSCT and CBCT devices

Equipment	Model Manufacturer	kVp	mA	t(s)	FOV WxLxH (cm ³)	Pixel Size (mm)
MSCT	Discovery 600 CT Lightspeed GE	120	99	5	70x70x*	0.35
FFOV-1	i-CAT Im.Sci.Int.	120	5	8	17x17x23	0.2
FFOV-2	9500 3D Kodak	90	10	10.8	18.4x18.4x20.6	0.3
FFOV-3	Orthophos XG 3D Sirona	85	7	5	8x8x8	0.16
SFOV-1	9000C 3D Kodak	70	8	10,8	5.0x5.0x3.7	0,076

C. Image Quality Analysis for CBCT Devices

The methodology developed for image quality analysis for CBCT devices is based on conventional CT QC procedures. The main properties and constrains of CBCT modality was considered in the phantom design. The physical parameters for image analysis and the proposed methodology are described below:

a) Uniformity:

CBCT devices image larger objects with a reduced FOV, resulting in increased scatter, and producing a negative impact on CT imaging performance by introducing non-uniformities in the reconstructed image, like cupping effect and streaks⁵.

The methodology proposed in this work to evaluate the uniformity avoids the reference ROI in the center of the FOV, and proposes the use of peripheral ROIs (anterior, lateral right and lateral left, related to the dental arcade) as references. This approach avoids the high influence of cupping in the uniformity measurement.

b) CT number Accuracy:

Our methodology proposes to build a fitting curve of CT numbers with different low and high density materials for each CBCT device, in order to correlate the measured values for conventional CT and those measured in CBCT.

c) Image Noise:

Most devices use kVp below 100, and a low mAs, resulting in higher image noise.

For image noise, the proposed methodology is similar to the QC procedure in conventional CT, calculating the

standard deviation of a uniform ROI, although this region should be limited to the diagnostic region of interest.

d) Contrast to Noise Ratio (CNR):

The first sector of the CBCT phantom was built to measure the contrast to noise ratio using low contrast (PMMA, PTEF, Delrin, and LDPE), and high materials (Al, air). The inserts consist of rods from 1.0 mm to 5.0 mm diameter inside a PMMA cylinder.

The methodology proposes to select appropriate exposure protocols according to the varying diagnostic requirements in dental practice. In each device, the minimum rods that will be visible are influenced by the radiation dose. The procedure allows distinguishing between the performances of CBCT devices' contrast resolution.

e) Spatial Resolution:

In CBCT devices, the spatial resolution is higher than in conventional CT, with pixel sizes generally below 4 mm, and nominally identical in all planes (isotropic).

The methodology to determine the spatial resolution is the calculation of the line spread function in an insert with a sharp edge of PMMA/PTFE interface.

f) Artifacts:

The methodology to estimate the metal artifact is to acquire an image in the insert which consists of a line of three 5.0 mm diameter titanium (Ti) rods suspended in PMMA. For measuring the extent of metal artifacts, a thresholding segmentation in the histogram maximum is used, and the ratio between white (related to metal and streaks) and black pixels (background) is determined. The value of this ratio increases when streaks originating from the metal object cover a larger area or when they are more pronounced

g) Geometric Distortion:

To evaluate the presence of geometric distortion, a line profile is obtained on the axial image of the third sector of the CBCT phantom, where an array of regularly deep air gaps is uniformly pitched throughout the phantom. The distance between air gaps is measured in different directions and compared in height and width to estimate distortion.

III. RESULTS

Uniformity and image noise were measured on the images obtained by scanning the second of the phantom. FOVs were placed at the periphery of CBCT phantom in the proposed methodology. Table 2 shows the comparison between uniformity ($|U|$) results, for MSCT and CBCT devices when the conventional methodology, using the central ROI as reference, and the proposed peripheral ROI as reference, are

used. The image noise (N), in the proposed method, uses the anterior ROI for estimation.

Table 2 Uniformity ($|U|$) and noise (N) measured on all devices using the conventional methodology and the proposed in this work.

Equipment	$ U _{\text{anterior}}$ (HU)	$ U _{\text{posterior}}$ (HU)	$ U _{\text{right}}$ (HU)	$ U _{\text{left}}$ (HU)	N (HU)
MSCT*	2.0	1.1	1.7	1.8	11.1
MSCT**	0.9	-	0.6	0.6	9.6
SFOV 1*	11.0	16.4	11.0	13,3	44.5
SFOV-1**	5.5	-	5.5	3.2	44.1
FFOV-1*	31.8	39.2	43.7	30,3	68.5
FFOV-1**	6.7	-	12.7	7.4	66.1
FFOV-2*	106.2	119.1	108.8	113.5	48.5
FFVO-2**	4.9	-	3.6	6.0	53.8
FFOV-3*	23.1	29.9	5.7	11.3	37.4
FFOV-3**	20.3	-	22.9	14.4	36.8

*Central ROI as reference; **Peripheral ROI as reference.

As expected, the uniformity parameter is lower for MSCT than in CBCT devices, and below the limits ($>10\text{HU}$) for conventional CT QC procedure. The measurement of uniformity in peripheral ROIs showed a non-uniform gray value distribution in all CBCT devices, when the reference ROI is the center of FOV. Bryant et al⁴ have shown the gradient of voxel values appearing for asymmetrical phantom positioning in a FFOV CBCT, leading to a decrease in uniformity throughout the entire volume.

Uniformity in CBCT shows large differences among devices. The conventional methodology (central ROI as reference) highlights the influence of cupping effect in CBCT FFOV devices. For the SFOV device, cupping effect is lower and this device shows the best result in uniformity among CBCT devices, for both conventional and proposed methodology. Among FFOV devices, FFOV-2 shows the worst result in uniformity ($>100\text{HU}$) using the conventional method, caused by the strong cupping effect in the central FOV (Figure 3). All FFOV CBCT devices show an improvement in uniformity index when a peripheral ROI (related to dental arcade) is used as reference. FFOV-3 uniformity image has a non-uniform CT number distribution between the left and right side, revealed by both methodologies.

Considering the peripheral region of clinical interest in dental applications, our methodology is reliable to be used to compare the uniformity among different CBCT devices.

The noise image parameter is lower for MSCT than in CBCT devices, due to the high-dose exposure. No significant difference was found when conventional or our methodology is used to estimate noise image.

Absolute values of CT numbers are affected by the amount of mass outside the reconstructed volume, producing inaccuracy in all CBCT devices. Table 3 shows the CT number for some materials and their percentage error, when multislice CT numbers are considered as reference.

Table 3 CT numbers and their errors, using MSCT as reference value.

Equipment	CT _{PMMA} (HU)	Error (%)	CT _{Al} (HU)	Error (%)
MSCT	126±25	-	2234±54	-
SFOV 1	136±60	-7.9%	992±82	55.6%
FFOV-1	102±93	19.0%	1648±138	26.2%
FFOV-2	142±43	-12.7%	1436±113	35.7%
FFOV-3	70±48	44.4%	743±78	66.7%

Highest CT numbers errors were observed in low density materials in FFOV devices. CT number variability increased when more objects were included outside the ROI area.

Figure 4 shows an example of correlation between CT number in MSCT and CBCT FFOV-2 device.

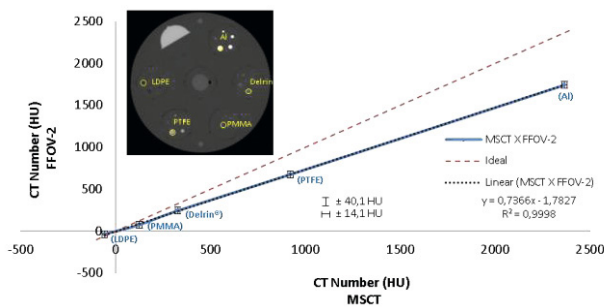


Fig. 4 Correlation between CT numbers in MSCT and FFOV-2 device.

The CBCT pixel values showed a strong linear correlation with MSCT. Similar findings were reported by Lagravère et al⁶ and Naitoh et al⁷.

CBCT devices show very poor soft tissue differentiation, because they are meant for hard tissue visualization (bone, teeth) and air (sinus and air cavities). CNR showed that noise is often similar or larger than the difference in mean CT value between LDPE and PMMA. With the aluminium insert, large differences in CNR were seen between devices.

A consistency was observed between spatial resolution values obtained from the ESF and voxel sizes of CBCT devices. Despite higher-dose protocols showed a higher spatial resolution, further studies are required to investigate additional factors, such as the influence of reconstruction algorithm and the surrounding presence of streak artifacts.

A method was established to quantify streaks from high-density and metal objects. Artifacts from titanium rods appeared different when comparing CBCT devices and protocols, but the values are highly affected by image noise.

The geometrical distortion was insignificant in all directions for all CBCT devices, using the recommended acquisition protocol.

IV. CONCLUSIONS

Based on the initial evaluations, the methodology was appropriate to evaluate image quality parameters for a wide range of CBCT devices. The CBCT phantom offers several structures for image quality assessment and can be optimized for evaluation of CBCT devices with different FOVs.

CONFLICT OF INTEREST

The authors declare that they have no conflict of interest.

REFERENCES

1. Miracle AC, Mukherji SK (2009) Cone beam CT of the Head and Neck, Part 1: Physical Principles. *AJNR* 30(6):1088-95.
2. Bamba J, Araki K, Endo A, Okano T (2013). Image quality assessment of three cone beam CT machines using the SEDENTEXCT CT phantom. *Dentomaxillofacial Rad*, 42(8):20120445.
3. Guerrero ME et al. (2006) State-of-Art on Cone Beam CT Imaging for Preoperative Planning of Implant Placement. *Clin Oral Invest* 10(1): 1-7.
4. Bryant JA, Drage NA, Richmond S (2008) Study of the Scan Uniformity from an i-CAT Cone Beam Computed Tomography Dental Imaging System. *Dentomaxillofacial Radiology*, 37(7):365-374.
5. Pauwels R, et al. (2011). Development and applicability of a quality control phantom for dental cone-beam J *App Clin Med Phys*, 12(4): 245-60.
6. Lagravère MO, et al (2008). Effect of Object Location on the Density Measurement and Hounsfield Conversion in a Newtom 3G Cone Beam Computed Tomography Unit. *Dentomaxillofacial Radiology*, 37(6):305-8.
7. Naitoh M, et al (2009). Evaluation of voxel values in mandibular cancellous bone: Relationship between cone-beam computed tomography and multislice helical computed tomography. *Clin Oral Implants Res*, 20(5):503-506.

Author: Elias C. Hoffmann
 Institute: PUCRS – Núcleo de Pesquisa em Imagens Médicas
 Street: Av. Ipiranga, 6681, Pr. 96A
 City: Porto Alegre
 Country: Brasil
 Email: elias.hoffmann@gmail.com